Exciton Dynamics of Photoexcited Pendant Porphyrin Polymers in Solution and in Thin Films

by

Amy L. Stevens[#], Sacha Novakovic[†], Jonathan M. White[†], Wallace W. H. Wong[†^],

Trevor A. Smith[†^], Kenneth P. Ghiggino[†^]*, Matthew F. Paige[#] and Ronald P. Steer[#]*

[#] Department of Chemistry,
University of Saskatchewan
Saskatoon, SK
Canada S7N5C9

[†]School of Chemistry and
[^]ARC Centre of Excellence in Exciton Science
University of Melbourne
Parkville, VIC 3010
Australia

*To whom correspondence should be addressed
ghiggino@unimelb.edu.au
ron.steer@usask.ca

Abstract:

Several new polymers with rotatable zinc porphyrin pendants have been synthesized and their optical spectroscopic and photophysical properties, including upconversion efficiencies, determined in both fluid solution and thin films. Comparisons made with the β-substituted zinc tetraphenylporphyrin monomers and ZnTPP itself reveal that the yield of triplets resulting from either Q-band or Soret-band excitation of the polymers is surprisingly small. A detailed kinetic analysis of the fluorescence decays and transient triplet absorptions of the substituted monomers and their corresponding polymers reveals that this phenomenon is due to two parallel internal singlet quenching processes assigned to transient intrachain excimer formation. Consequently, the yields of upconverted S_2 fluorescence resulting from Q-band excitation in the degassed polymers are significantly diminished in both fluid solution and thin films. Implications of these results for the design of polymer upconverting systems are discussed.

Introduction:

Acquiring sufficient knowledge to enable control of the dynamics of excitons produced in electrically and optically excited materials has been a goal of researchers for several decades.[1] Studies of the behaviour of excitons in nanoparticles,[2] quantum dots[3,4] and polymers[5] have been particularly prominent recently. For organic materials, applications in organic photovoltaics (OPVs), organic light emitting diodes (OLEDs) and organic field effect transistors (OFETs) are being pursued vigorously.[1,6,7]

Metalloporphyrins are particularly attractive as excitonically-active materials in photo-excited systems.[8,9] Their absorption spectra span the visible spectrum and can be extended well into the near infrared by appropriate synthetic modification, thereby providing excellent solar energy capture possibilities. Porphyrinoids generally exhibit high intersystem crossing yields and unusually long triplet lifetimes in deoxygenated media, making them ideal for use in both sensitizer and upconversion applications.[10] Many fluoresce detectably from both their first and second excited singlet states, providing experimental access to their singlet exciton migration and decay kinetics in a variety of media and for a wide range of excitation wavelengths.[11] Triplet transient absorption information can usually be obtained straightforwardly,[10] and some heavy atom-containing species exhibit readily measurable phosphorescence even at room temperature,[12] thus allowing triplet exciton kinetic data to be secured.

A wide variety of multimeric porphyrins have been synthesized, often with a view to seeking insight into exciton migration and thus establishing useful structure-dynamics relationships. Both self-aggregated and covalently linked multimers have been examined.[13,14] Prominent among stable covalently-bound materials examined to date are: (i) porphyrin tapes[15]

in which monomers are either linked via their *meso*-positions or fused through their β-β positions, (ii) dendritic porphyrins[16] and (iii) pendant porphyrin polymers.[17] The latter group of polymers is of particular interest because of the wide variety of structural nuances that may be incorporated in them, including the number, spacing and geometric orientation of the pendant chromophores. Thus, rapid exciton migration has been observed in helical polyisocyanides[18] with closely-spaced pendant zinc and free-base porphyrins, and ultrafast singlet-singlet and singlet-triplet exciton annihilation have been recorded in porphyrin-pendant cyclobutene and norbornene ring-opened polymers having a variety of Z/E conformations.[19]

In our laboratories, we have been particularly interested in the dynamic effects of the aggregation of exciton-carrying species, both in solution and in thin films, with particular emphasis on applications in non-coherent photon upconversion (NCPU) by triplet-triplet annihilation (TTA).[20,21] In particular we have discovered that the efficiencies of TTA in zinc porphyrins, where S_2 is the initially-produced upconverted state, are controlled by geometric factors not accounted for in simple Dexter, electron-exchange theory.[22] Surprisingly, these efficiencies are significantly diminished when upconversion occurs at the van der Waals separations normally found in ground state dimers,[23] and rise to an optimum when porphyrin substitution produces sufficient steric crowding to extend the interaction distance.[22]

Our work on $Ru(dmbpy)_3$-sensitized pendant diphenylanthracene (DPA) polymers[24,25] has revealed a pathway for rapid triplet bi-exciton annihilation in single polymer chains. Although a minor contributor to the overall exciton decay dynamics, this rapid bi-excitonic decay process reveals the possibility of designing multi-chromophoric polymers that produce

upconverted electronic states on a time scale much faster than achievable by normal intermolecular exciton diffusion processes.

As part of a larger scale study of exciton dynamics in polymeric materials, we report here the photophysics of several pendant zinc porphyrin polymers synthesized in-house to reveal the structural designs that may be required to produce upconverted electronic states more rapidly than is possible by more conventional intermolecular triplet-triplet diffusional processes. We monitor the polymer exciton dynamics by observing transient triplet absorption, S_1 fluorescence and S_2 fluorescence produced by direct excitation and both interchain and intrachain TTA. The tethered photo-excited monomers and unsubstituted zinc tetraphenylporphyrin (ZnTPP) serve as model controls.

Experimental:

Materials:

Monomeric derivatives of ZnTPP and the polymers derived from them were all synthesized in-house using methodology that has been described previously.[26] Full synthesis and characterization details are provided in the Supporting Information. Briefly, three sets of β-substituted zinc porphyrins and their pendant porphyrin polymers were synthesized; one using a *para*-substituted diphenyl ether link (and therefore not conjugated with the macrocycle), and two using *meta*- and *para*-substituted styrene links (both of which are conjugated with the macrocycle). The porphyrin polymers were synthesized by post-polymerization functionalization of a low polydispersity RAFT polymer to produce linear chains with an average

26-pendant porphyrin structure. The structures of the monomers used as model compounds and the polymers derived from them are shown in Scheme 1.

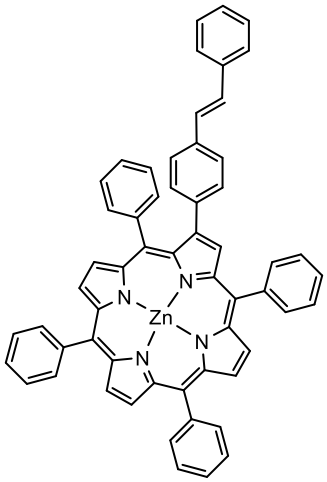

p-SL mon

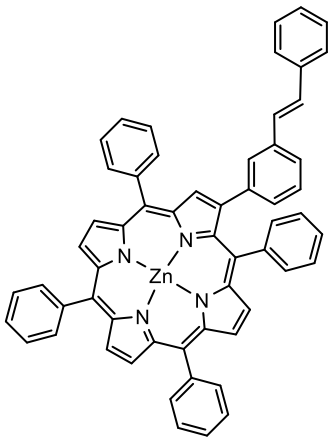

m-SL mon

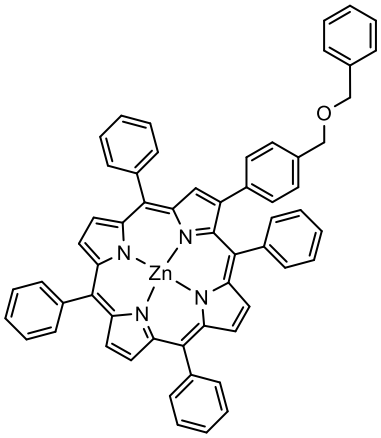

p-EL mon

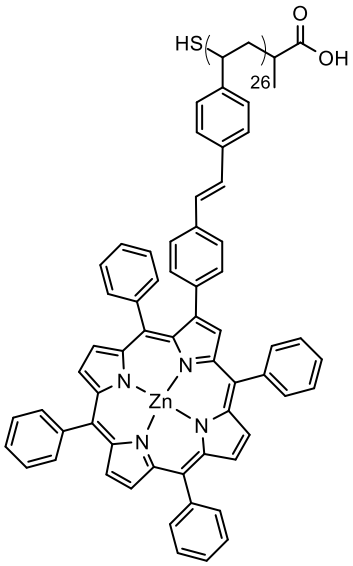

p-SL pol

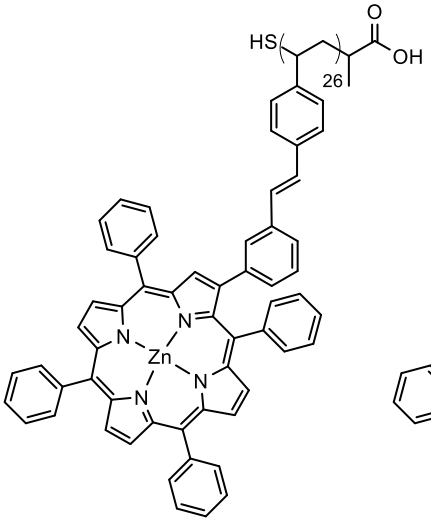

m-SL pol

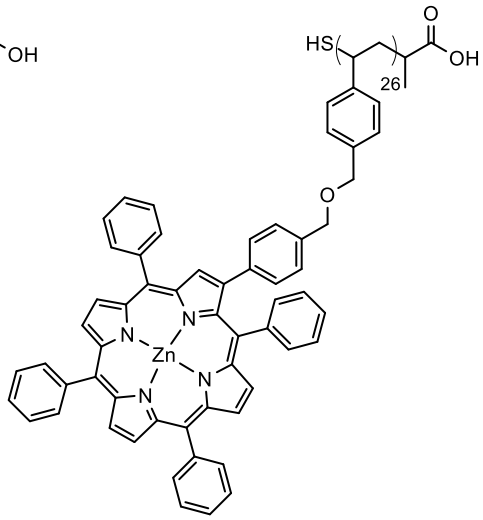

p-EL pol

Scheme 1: Structures for the porphyrin polymers (pol) and monomer (mon) models synthesised and investigated. SL is styrene linked; EL is ether linked.

Techniques:

All experiments were performed at room temperature. Repeated freeze-pump-thaw cycles on a vacuum line were used when degassing was required. Descriptions of the controls and corrections used to obtain reproducible quantitative results from the spectroscopy and kinetics measurements are provided in the Supporting Information.

Absorption spectra were recorded on a Cary 6000i UV-Vis-NIR or a Varian Cary 50 Bio spectrophotometer using 10 mm or 1 mm pathlength quartz cells. Steady state fluorescence emission measurements and TTA-UC experiments were carried out using a custom-modified SPEX Fluorolog spectrofluorometer, as previously described.[27] Excitation sources were 405 nm and 532 nm cw lasers, the output of which passed through one of a set of neutral density filters on a filter wheel to obtain variable excitation powers. Excitation powers were measured at the cell face with a power meter. When required, a notch filter was employed to eliminate excitation scatter from the emission spectra. When comparing emission intensities, solute concentrations were adjusted to give nearly identical absorptivities at the excitation wavelength, and any small deviations from identical absorptivity were corrected by proportionation. Emission from the S_2 state was corrected for reabsorption due to the strongly-overlapping Soret absorption band by methods previously described.[28]

Thin-film samples, some diluted by PMMA, were drop-cast from toluene on 2.5 cm glass discs that had been precleaned using a plasma cleaner. The TTA experiments on these samples were conducted by using the coated discs as the front-face window of an evacuable metal cell, with the sample on the high-vacuum side and intercepting the incoming laser beam at 45^o as previously described.[29]

Nanosecond fluorescence lifetimes of the S_1 states were measured by time-correlated-single-photon-counting using magic angle excitation of the sample by frequency doubled mode-locked 400 nm pulses from a Ti:sapphire laser (Coherent, Mira) as described previously.[30] The instrument response function was obtained by scattering from a Ludox solution and exhibited a typical FWHM of *ca*. 50 ps.

Transient triplet spectra and decay kinetics were measured using an Edinburgh Instruments LP920 nanosecond flash photolysis system using the second harmonic output of a Qantel Brilliant B Nd:YAG laser for excitation (10 ns pulse width, λ_{exc} = 532 nm, 1.2 to 8.2 mJ pulse energy).[31] Full instrument and data analysis details are provided in the Supporting Information.

Results and Discussion:

The UV-visible absorption spectra of the *p*-ether-linked zinc porphyrin monomer, its corresponding polymer, and the model monomer ZnTPP, each in toluene, are shown in Figure 1. Their measured molar absorptivities at the band maxima and at the 532 nm excitation wavelength used for many experiments are given in Table 1. (Similar data for the other polymers and monomers are provided in the Supporting Information.) Note that the molar absorptivity of the polymer is given on a per pendant porphyrin basis, based on a mean of 26 pendants per polymer chain. The spectra shift slightly to the red and broaden when ZnTPP is tethered by β-substitution of the pendant, and a slightly larger red shift and broadening is found in the polymer as compared with the monomer. However, of importance, there is very

little evidence in the polymer absorption spectra of excitonic splitting due to electronic interactions among the pendant porphyrins.

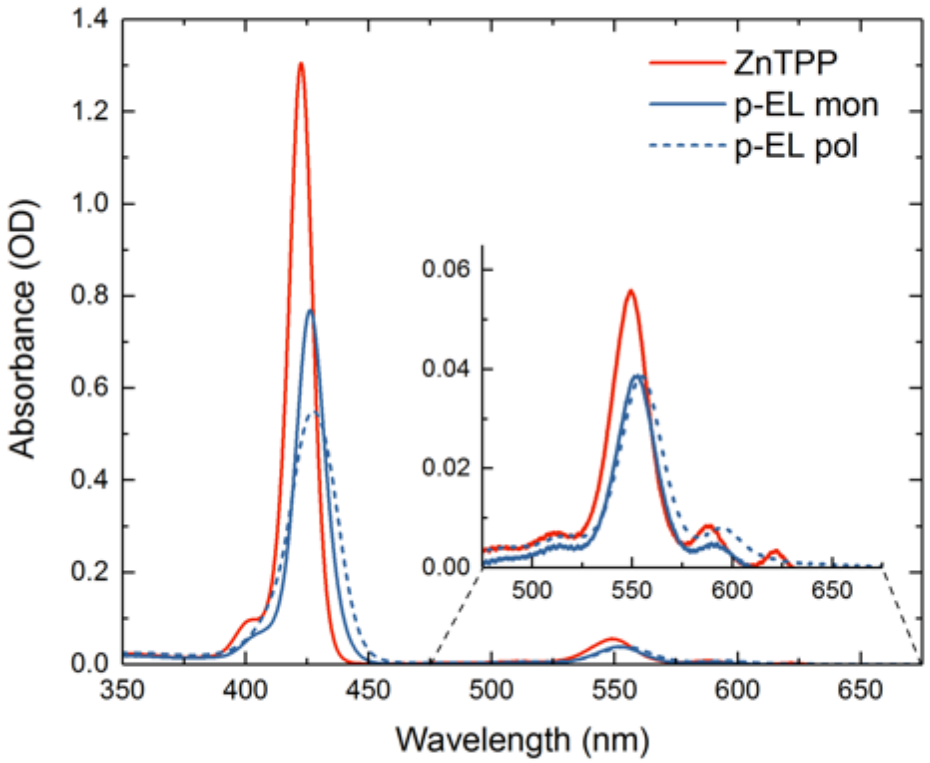

Figure 1 : UV-visible absorption spectra of the *p*-ether-linked polymer (blue dashed line), the *p*-ether-linked monomer (blue solid line) and the model monomer, ZnTPP (red) in toluene at concentrations of 2 µM at room temperature. The inset provides an expanded view of the Q band absorption. As described in the text, the polymer absorbance is per porphyrin pendant.

Table 1: Molar absorptivities of ZnTPP, the ether-linked monomer and its polymer at their band maxima and at 532 nm in toluene

Compound	Soret λ_{max} (nm)	Soret ε ($M^{-1}cm^{-1}$)	Q-band λ_{max} (nm)	Q-band ε_{max} ($M^{-1}cm^{-1}$)	Q-band ε_{532} ($M^{-1}cm^{-1}$)
ZnTPP	423	5.48×10^5	550	2.36×10^4	6.95×10^3
ether monomer	426	4.37×10^5	553	2.26×10^4	4.77×10^3
ether polymer*	429	2.39×10^5	555	1.61×10^4	3.47×10^3

* Molar absorptivities are per porphyrin pendant.

Direct one-photon excitation in the polymer and monomer Q and Soret bands produces readily observable fluorescence from their lowest excited singlet states, S_1. Consistent with previous measurements on diamagnetic metalloporphyrins containing low atomic mass metal ions,[11, 28] direct excitation of both the monomers and polymers in the Soret region also produces very weak fluorescence from the next highest excited singlet, S_2, as shown in Figure 2. Fluorescence quantum yields from both the S_1 and S_2 states when directly excited in the Soret band near 405 nm and from S_1 when excited in the Q band at 532 nm are collected in Table 2.

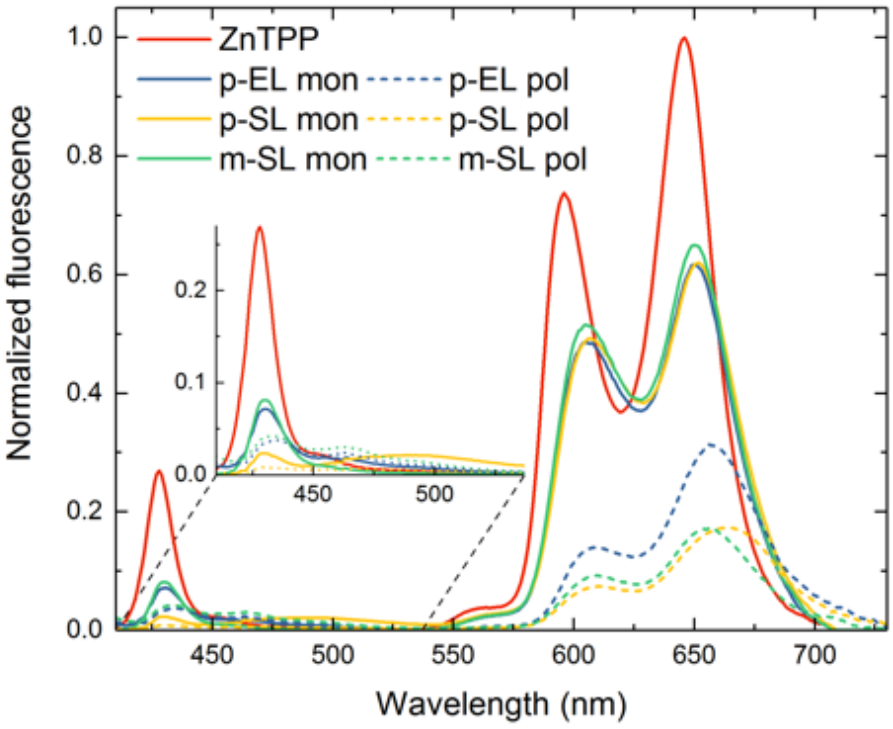

Figure 2: Fluorescence from the three pendant porphyrin polymers and the corresponding monomers (in toluene) excited at 405 nm, all at the same absorbance. ZnTPP in toluene (red) is used as a reference for determining relative intensities. S_1 fluorescence spectra excited at 532 nm are given in Figure S4 in the Supporting Information.

Table 2: Fluorescence quantum yields, excited at 405 nm and 532 nm.

Samples	**F***	**ϕ_f (S_2-S_0)/10^{-3}** S_2-S_0 (410 to 537 nm)	**ϕ_f (S_1-S_0)/10^{-2}** S_1-S_0 (537 to 736 nm)
405 nm			
ZnTPP at 2 μM	0.892	1.14 ± 0.02#	2.93 ± 0.03#
p-EL mon at 2.8 μM	0.892	0.54 ± 0.02	2.21 ± 0.03
p-SL mon at 2.5 μM	0.900	0.46 ± 0.01	2.29 ± 0.03
m-SL mon at 1.9 μM	0.895	0.39 ± 0.01	2.33 ± 0.03
p-EL pol at 0.1 μM	0.892	0.50 ± 0.01	1.06 ± 0.06
p-SL pol at 0.1 μM	0.891	0.15 ± 0.01	0.65 ± 0.06
m-SL pol at 0.1 μM	0.893	0.62 ± 0.03	0.60 ± 0.09
532 nm			
ZnTPP at 15 μM	0.846	-	2.93 ± 0.03#
p-EL mon at 29 μM	0.824	-	2.3 ± 0.1
p-SL mon at 27 μM	0.854		2.46 ± 0.03
m-SL mon at 19 μM	0.861		2.47 ± 0.03
p-EL pol at 1.0 μM	0.795	-	2.1 ± 0.1
p-SL pol at 0.9 μM	0.884		1.3 ± 0.1
m-SL pol at 1 μM	0.867		1.1 ± 0.1

* The fluorescence reabsorption correction factor F is given by $F = (1\text{-}10^{-(Aexc)})/(2.303A_{exc})$.
# ZnTPP is used as an internal standard. Intensities are normalized to the same absorbance at the excitation wavelength when calculating the quantum yields. Data are from reference 32.

Note that the substituted monomers produce slightly smaller quantum yields of both S_1 and S_2 emission than ZnTPP, an effect that can be attributed to slightly increased rates of radiationless decay associated with substitution at the β-position of the porphyrin macrocycle. The corresponding polymers produce still smaller, but nevertheless readily measurable

quantum yields of emission, again indicating that the ratios of the rates of radiationless to radiative decay become still larger in the polymers. Note also that the quantum yield of S_1 fluorescence of the *p*-ether-linked monomer decreases by only a few percent when excited at 405 nm compared with 532 nm (absorbances are matched for each excitation wavelength), whereas for the corresponding polymer this decrease is about a factor of two. These important measurements indicate that: (i) like ZnTPP itself,[32] the $S_2 - S_1$ internal conversion efficiencies of the monomers are near unity, and (ii) in the pendant polymers self-quenching of the S_2 excited states directly to the ground states accounts for about one half of the radiationless decay. A radiationless decay process that is not present in the β-substituted monomers contributes strongly to the relaxation of the corresponding polymer (*vide infra*).

Figures 3 and 4 show that S_2 fluorescence is also produced when the *p*-ether-linked monomer and polymer are excited in the Q band at 532 nm in deaerated toluene solution as a result of NCPU by TTA. Oxygenation eliminates this emission, proving that the upconversion process involves the porphyrin triplet states. Note in particular the near linear dependence of the weak upconverted emission intensity of the polymer on the incident 532 nm laser power (*vide infra*). A quadratic power dependence of the upconverted emission intensity is expected at the lowest of the powers employed,[20] and this is seen in the monomers (Supporting Information, Figure S7) but not the polymer.

Figure 4 also demonstrates the effect of the coordinating solvent, THF, on the NCPU efficiencies of both the *p*-ether-linked monomer and the *p*-ether-linked polymer. Axial coordination of the THF at the zinc centers of the porphyrin frustrates the close approach of triplet pairs needed for efficient TTA. The ratio of the TTA-produced S_2 emission intensities in

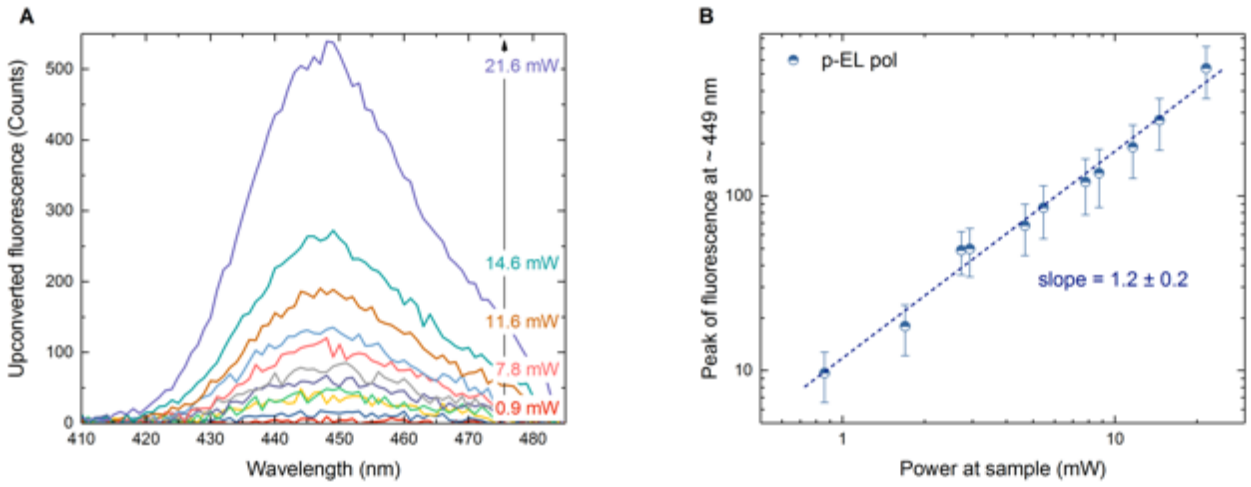

Figure 3: (A) NCPU by TTA for a 1 μM sample of the *p*-ether-linked polymer in degassed toluene excited at 532 nm; (B) Power dependence of the upconverted emission intensity. The power dependence of the upconverted emission intensity of the monomer is given in Figure S7.

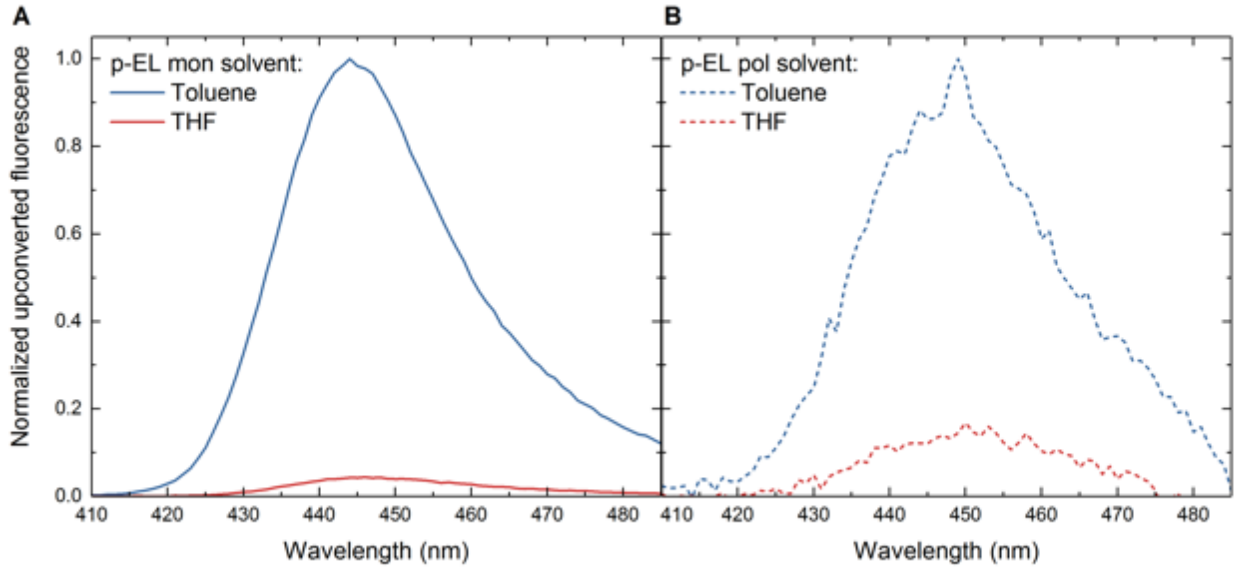

Figure 4: Comparison of the relative NCPU emission intensities in degassed toluene and the degassed coordinating solvent, THF, for the *p*-ether linked monomer (A, area ratio = 22) and the *p*-ether-linked polymer (B, area ratio = 6.5). Excitation is at 532 nm. The emission spectra of the polymer in both solvents are shown in Figure S5.

toluene (non-coordinating) *vs.* THF (coordinating) is 22 for the monomer, identical to that observed previously for the unsubstituted ZnTPP monomer in the same and similar solvents.[29] This ratio falls to *ca.* 6 for the polymer, suggesting that a significant fraction of the TTA interactions in the excited polymer solutions are unaffected by solvent coordination. We posit that the quantitative difference between the solvation behaviour of the model monomers and the polymer is caused by an intertwining of the polymer chain(s) that blocks full solvent access.

The quantum yields of fluorescence resulting from TTA may be obtained by using ZnTPP as a standard, for which the NCPU S_2 fluorescence quantum yield is 1.5×10^{-4} in degassed toluene at room temperature.[33] Measuring the S_2 fluorescence intensity for the monomers and polymers in degassed toluene and comparing them with that from ZnTPP at similar absorbed power density allows the upconversion quantum yields to be assessed. The largest of the set of very small quantum yields of upconverted S_2 fluorescence (*cf*. Supporting Information, Table S1) are provided by the *p*-ether-linked monomer ($\phi_{UC} = 2.3 \times 10^{-5}$) and its corresponding polymer ($\phi_{UC} = 4 \times 10^{-7}$), yielding ($\phi_{UC}$, monomer/$\phi_{UC}$ polymer) = 58.

These observations lead to two important conclusions. First, porphyrin polymers of the type examined in this study will be unsuitable for use as efficient dual absorber-upconverters in photon-activated systems; the yield of the upconverted S_2 state is too small for efficient electronic energy or electron transfer to take place. Second, the linear power dependence of the upconverted steady-state emission in the polymer (but not the monomers) suggests that the mechanism of TTA in the polymer must differ from that which applies to the monomers. A linear power dependence of the upconverted emission intensity would normally be expected

only if a large majority of triplets are consumed via TTA – usually seen only in the high power density limit.[20] Such is clearly not the case for the power densities used to obtain Figure 3B.

The nanosecond decay kinetics of the S_1 states of all species were determined with 50 ps precision by time-correlated single photon counting of Q band fluorescence following ps pulsed laser excitation in the Soret band. Typical decay curves are shown in Figures 5 and S6, and the decay parameters obtained from single and multi-exponential fits of the data are given in Table 3. Note that the β-linked monomers all exhibit identical monoexponential decays with lifetimes of 1.55 ns, slightly shorter than that of the unsubstituted compound, ZnTPP, as expected. Together with the S_1 fluorescence quantum yield data of Table 2, the substituted monomers yield values of the S_1 radiative and non-radiative decay constants; $k_r = (1.5\pm0.2) \times 10^7\ s^{-1}$ and $k_{nr} = (6.3\pm0.3) \times 10^8\ s^{-1}$ respectively. The polymer decay data are better fit by multi-exponential decays, also as expected if the pendant porphyrin chromophores are absorbing independently and experience different local environments during their lifetime. The measured decay time for ZnTPP in toluene is in agreement with previous reports.[28, 30] Bi-exponential fits of the polymer fluorescence decay data are satisfactory and reveal a minor component similar to that of the monomer, *ca.* 1.55 ns, together with a major component of *ca.* 0.5 ns, roughly one third of the monomer's lifetime. These observations, together with data detailing the much lower net yields of triplets in the excited polymer (*vide infra*) suggest that a substantial fraction of the initially excited singlet states of the polymer decay directly to the ground state via one or more self-quenching mechanisms.

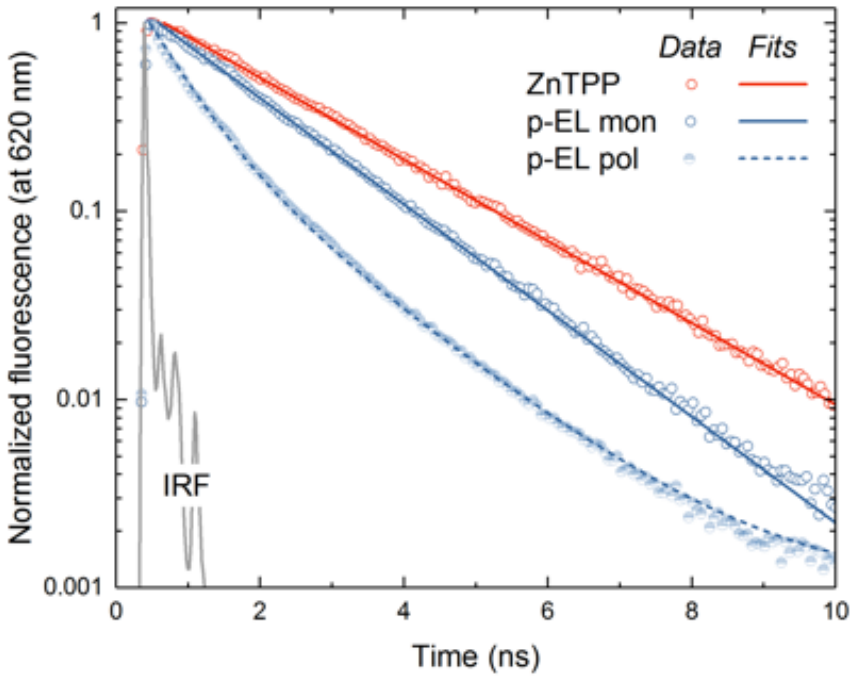

Figure 5: Normalized fluorescence decay curves for ZnTPP, the *p*-ether-linked zinc porphyrin monomer and the corresponding polymer each 2 μM in toluene at room temperature. Excitation at 400 nm; detection at 620 nm; > 10^4 counts in the peak channel. IRF is the instrument response function.

Table 3: S_1 Fluorescence decay parameters of solutes in toluene at room temperature.

Sample **Q band excitation**	**τ_1 (ns)**	**α_1**	**τ_2 (ns)**	**α_2**	**R^{2*}**
ZnTPP	2.00 ± 0.06	1.00			0.988
p-EL monomer	1.54 ± 0.04	1.00			1.000
p-EL polymer	0.57 ± 0.02	0.71	1.51 ± 0.07	0.29	0.999
p-SL monomer	1.55 ± 0.05	1.00			0.999
p-SL polymer	0.47 ± 0.02	0.86	1.49 ± 0.05	0.14	0.998
m-SL monomer	1.55 ± 0.03	1.00			0.998
m-SL polymer	0.52 ± 0.04	0.81	1.55 ± 0.05	0.19	0.999

* Monomer data are fit with a monoexponential decay function; polymer data with a biexponential function.

Transient triplet spectra and triplet decay kinetics as a function of excitation power were measured for all samples in toluene and for several samples in THF. The triplet absorption spectra are shown in the Supporting Information (Figure S8). Typical triplet temporal decay profiles, measured at the triplet absorption maximum near 470 nm are shown in Figure 6, and a time-expanded view of the first few microseconds of the polymer decays at three different excitation powers is given in Figure 7. The monomer triplet decays in degassed solution can be modeled satisfactorily by parallel kinetically first and second order (in triplet) processes, with the second order process, TTA, contributing only a small fraction of the overall triplet decay. In detail, the important steps in the kinetic mechanism for the monomer, (M), are as follows:

$M(S_0) + h\nu_{532nm} \rightarrow M(S_1)$	I_a
$M(S_1) \rightarrow M(S_0) + h\nu_f$	ϕ_f
$M(S_1) \rightarrow M(T_1)$	ϕ_{isc}
$M(T_1) \rightarrow M(S_0)$	k_1
$M(T_1) + M(T_1) \rightarrow M(S_2, T_n) + M(S_0)$	k_2
$M(S_2) \rightarrow M(S_1) \rightarrow M(T_1)$	$\phi_{T1} < 10^{-3}$

This kinetic scheme results in a combined 1st and 2nd order decay function for the analysis of the triplet-triplet transient absorption profile:

$$\Delta OD(t) = \varepsilon_{T1} \cdot \frac{[C_0]e^{-k_1 t}}{1+\frac{k_2}{k_1}[C_0]-\frac{k_2}{k_1}[C_0]e^{-k_1 t}} \quad (1)$$

where ε_{T1} is the triplet-triplet extinction coefficient and $[C_0]$ is the initial concentration of triplets. The fits of this function to the triplet decay data for the *p*-ether-linked monomer excited with 10 ns pulses of 532 nm laser radiation with energies of 1.2 mJ, 3.9 mJ and 8.2 mJ

are shown in Figure 8. A value of k_1 = 4.1 x 10^3 s^{-1} is obtained (*i.e.* a triplet lifetime of *ca.* 240 μs). A value of k_2 = 7.9 x 10^9 $M^{-1}s^{-1}$ is then calculated assuming a literature value of ε_{T1} = 7.16 x 10^4 $M^{-1}cm^{-1}$ for the ZnTPP triplet at its absorption maximum of 470 nm.[34] This value of k_2 suggests that the TTA process in the porphyrin model monomer is diffusion controlled. The rate constant for the production of the upconverted, unquenched S_2 state would be ¼ of k_2, as required by spin statistics and previously observed for ZnTPP in toluene.[33] The value of k_1 is similar to those previously measured for other β-monosubstituted ZnTPP triplets in degassed toluene.[35]

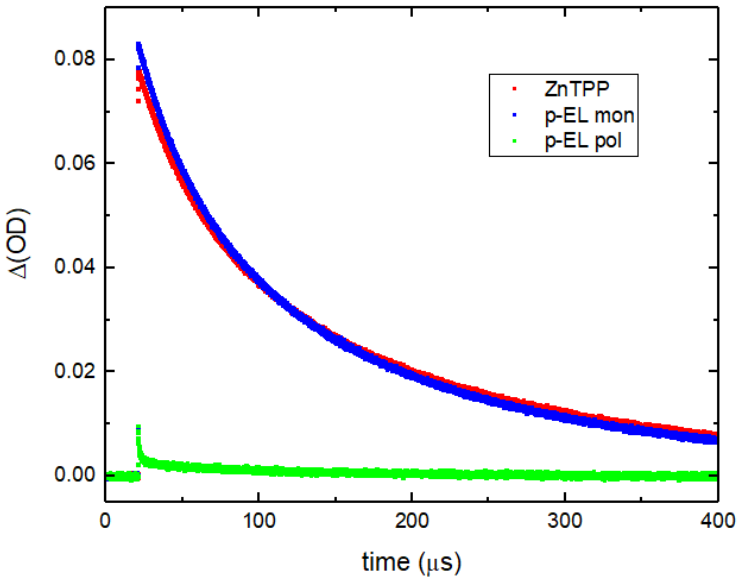

Figure 6: Triplet transient decays of ZnTPP (blue), the *p*-ether-linked monomer (red) and the *p*-ether-linked polymer (green) all in degassed toluene at room temperature. Excitation was at 532 nm and the triplet absorptions were monitored at the strong triplet absorption band maxima near 470 nm. The transient spectra are in the Supporting Information, Figure S8.

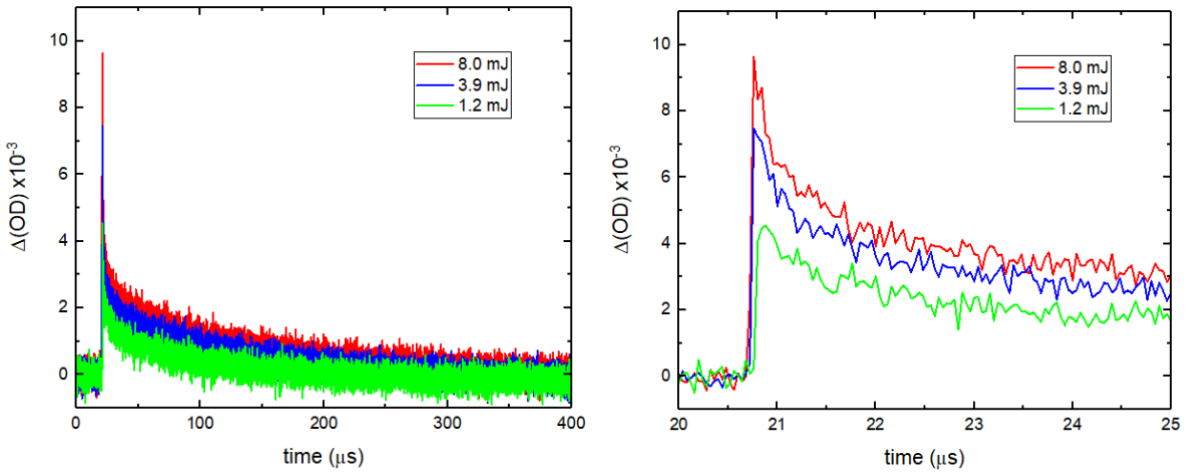

Figure 7: Decays of the polymer transient triplet absorption in degassed toluene for three different excitation pulse energies. The transient spectra are in the Supporting Information, Figure S8

.

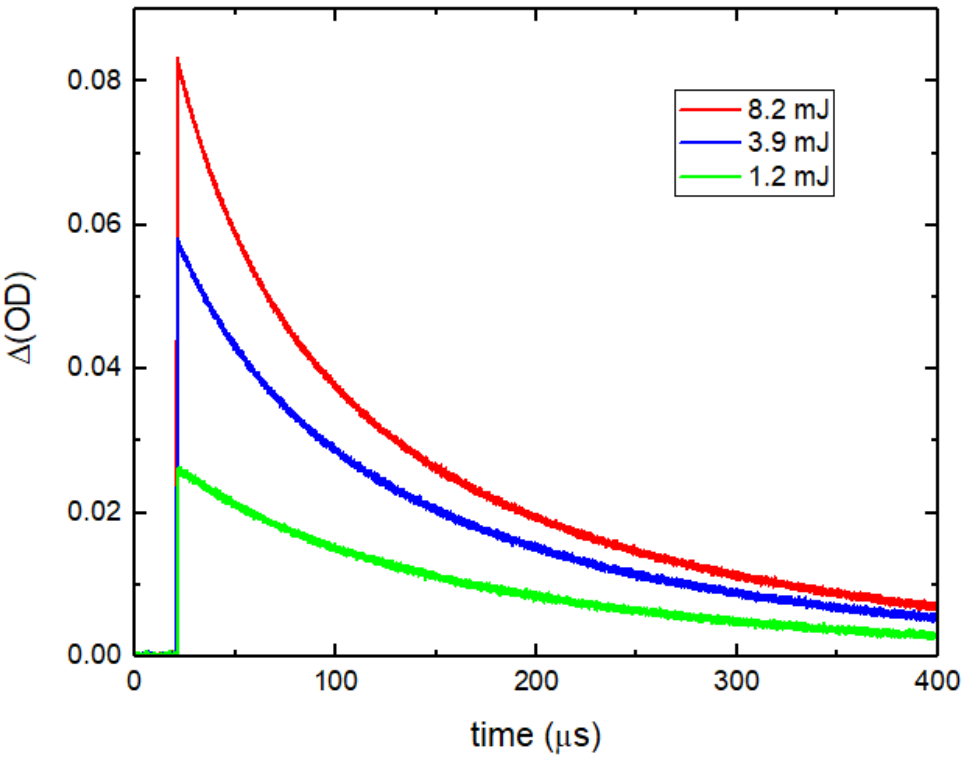

Figure 8: The triplet decay data for the *p*-ether-linked monomer excited at 532 nm with 10 ns pulses of 1.2, 3.9 and 8.2 mJ pulse energies.

The fractional contribution of the 1st and 2nd order components to the total triplet decay profile described by equation 1 can be estimated in the following manner. The integrated area under the decay curve due to the 1st order component can be estimated by simulating the 1st order decay using the best fit parameters (ε_{T1}, $[C_0]$ and k_1 in $I(t) = \varepsilon_{T1}[C_0]\exp(-k_1t)$) from the combined equation. The simulated single exponential decay is normalised to the experimental decay data at very long times (where the 2nd order contribution should be negligible) and the area under the resultant decay curve is calculated (A/k_1). The integrated area under the total decay curve is corrected due to the truncation of the decays by adding the difference in areas calculated by summing the data numerically and algebraically from A/k_1. The fractional contribution of the 1st order component to the total triplet decay profile is then calculated by dividing the area calculated from A/k_1 by the corrected integrated area under the total decay curve. The results of this analysis are provided in Table 4.

Table 4: Kinetic parameters obtained from the *p*-ether monomer transient triplet absorption experiments in degassed toluene. ε_{T1} = 71,600 M^{-1}; F_1 and F_2 are the fractional contributions to the total triplet decay profile of the 1st and 2nd order components.

Excitation Power (mJ)	**$[C_0]$ (M)**	**F_1**	**k_1 (s^{-1})**	**F_2**	**k_2 ($M^{-1}s^{-1}$)**
1.2	3.7×10^{-7}	0. 80	4.1×10^{3}	0.20	7.9×10^{9}
3.9	7.2×10^{-7}	0.74	4.1×10^{3}	0.26	7.9×10^{9}
8.2	1.16×10^{-6}	0.71	4.1×10^{3}	0.29	7.9×10^{9}

Two prominent differences are observed in the polymer *vs.* monomer triplet decay data. First, the yields of polymer triplet are small – less than *ca*. 10% of the yields of the monomer triplet under the same excitation conditions. Second, the polymer triplet exhibits additional decay processes, absent in the monomer (*cf*. Supporting Information, Figure S9), that appear

prominently in the first few microseconds of its decay. We propose the following mechanism to account for these interesting aspects of the polymer's triplet decay and the small triplet yield.

Consider $P_n(X)$, a single polymer molecule, numbered n, for which one pendant is initially excited to its lowest excited singlet state. If isolated from other porphyrins such excited pendants may behave much like the excited monomers, fully solvated and relaxing primarily by intersystem crossing to the ground state as described by equation (1A) (*cf*. the following mechanism). However unlike the monomers, more than 90% of the polymer S_1 decay must bypass T_1, either by enhanced internal conversion, 1B, or by other mechanisms. Here, we suggest that an excited polymer pendant may interact with other neighbouring pendants on the same chain during its nanosecond lifetime as a result of rotation about the polymer backbone. The excited species can thus be quenched rather efficiently by a transient intramolecular excimer-forming mechanism, as described by equations 2A and 2B, and similar to that previously observed by Fox and coworkers in other polymer systems.[36] Such a mechanism would be consistent with the lack of significant excitonic splitting in the polymer Soret spectra. Such splitting would require constant interaction of the pendants given the sub-picosecond lifetimes of the S_2 states. Finally, the excited polymer pendant may weakly interact with porphyrin pendants on other polymer molecules (or perhaps intramolecularly with non-adjacent pendants at folds[36]) as described by equations 3A and 3B.

$$P_1(S_0) + h\nu_{532} \rightarrow P_1(S_1) \rightarrow P_1(T_1) \rightarrow P_1(S_0) \qquad (1A)$$

$$P_1(S_1) \rightarrow P_1(S_0) \qquad (1B)$$

$$P_1(S_1)\ldots P_1(S_0) \rightarrow P_1(T_1)\ldots P_1(S_0) \rightarrow P_1(S_0) + P_1(S_0) \qquad (2A)$$

$$P_1(S_1)\ldots P_1(S_0) \rightarrow P_1(S_0)\ldots P_1(S_0) \qquad (2B)$$

$$P_1(S_1) + P_2(S_0) \rightarrow P_1(T_1)\ldots P_2(S_0) \rightarrow P_1(S_0) + P_2(S_0) \qquad (3A)$$

$$P_1(S_1) + P_2(S_0) \rightarrow P_1(S_0) + P_2(S_0) \qquad (3B)$$

Equation 1A represents the decay route of an isolated excited singlet porphyrin pendant that yields the longest-lived and by far the largest fraction of the *observed* triplet decays (but accounts for less than 10% of the S_1 decays). Equations 2A/2B and 3A/3B represent pairs of kinetically competitive pseudo-first order processes in which the yields of triplet are small ($k_{2B} >> k_{2A}$ and $k_{3B} >> k_{3A}$) and which generate triplets that initially decay faster than those represented in equation 1A. Processes 1B, 2B and 3B account for the relatively small yields of triplets in the pendant porphyrin polymers. Thus this mechanism predicts that the *observed* triplets of the polymer will decay by three parallel kinetically first order processes, with the decays of the isolated triplets dominating. In non-coordinating solvents such as toluene, the triplet decay rate within process 1, i.e. $P_1(T_1) \rightarrow P_1(S_0)$, is $k_1 = 3.82 \times 10^3\ s^{-1}$, which is obtained from best first order kinetics fit of the triplet decay data at long times after excitation.

Fits of this mechanism to the data for the two minor but faster pseudo-first order components of the triplet decay (2A and 3A) are excellent and are shown in Figure 9. This parallel first order triplet decay mechanism then yields values of $k_{2A} = (2.32 \pm 0.24) \times 10^6\ s^{-1}$ and $k_{3A} = (1.86 \pm 0.10) \times 10^7\ s^{-1}$, with process 2A accounting for a larger fraction of the fast triplet decays at higher excitation powers.

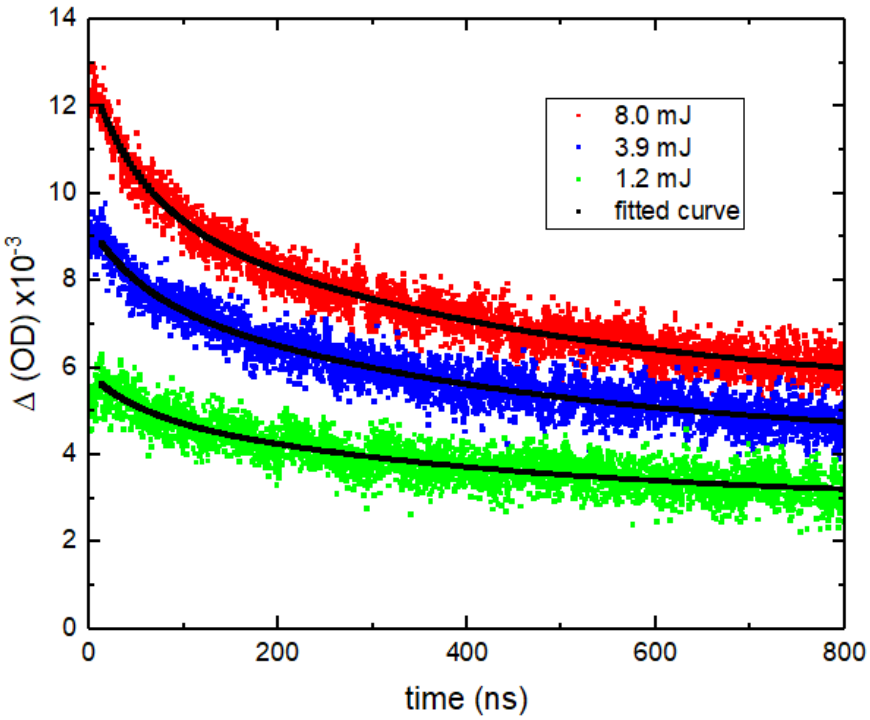

Figure 9: Fits of the data with the proposed mechanism for the decays of the polymer triplets in the *p*-ether-linked polymer on a microsecond time scale. The three traces are for excitation pulse energies of 8.0 mJ (top), 3.9 mJ (middle) and 1.2 mJ (bottom).

The yield of triplets is relatively small in the polymer, and only a tiny fraction of triplets in this scenario undergo TTA and produce observable upconverted S_2 fluorescence (*cf*. Table S1, Supporting Information). Thus, unlike the monomers, a second order annihilation process would have no observable effect on the polymer triplet decay kinetics as displayed by the transient triplet absorption experiments. However, the effect of solvation by coordinating solvents such as THF on the TTA rate is nevertheless seen in the reduction of the steady-state upconverted S_2 emission intensity in degassed solutions. The coordinating solvent curtails the rate of the bi-excitonic interaction, largely involving the freely solvated pendants, but not others buried within the polymer structure.

Attempts were made to increase the yield of upconverted emission by performing similar sets of both CW and pulsed laser experiments on the monomers and their polymers in thin films. These films were drop-cast with and without the use of PMMA as a possible solute diluent, again using ZnTPP as a model. Typical data from CW-excitation are shown in Figure 10. Upconversion in the polymer was barely observable under any of the conditions employed and was difficult to reproduce. The results for the monomers were unremarkable and followed the trends established previously for ZnTPP in similar matrices.[37]

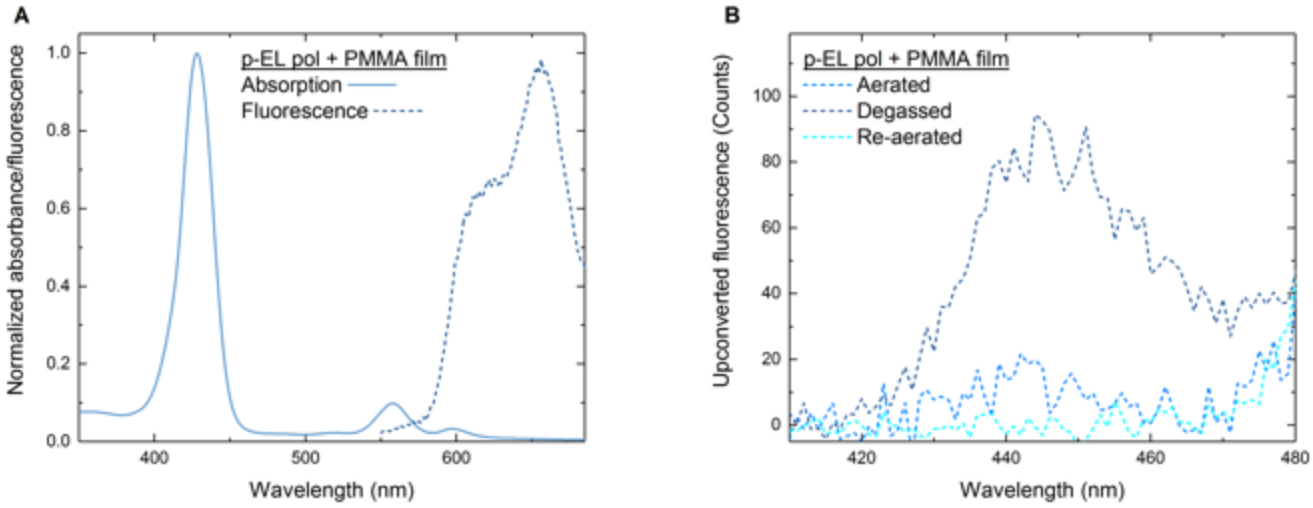

Figure 10: (A) Absorption annd emission spectra in PMMA and; (B) upconverted emission spectra excited at 532 nm for the *p*-ether-linked polymer in PMMA film.

Conclusions:

The photophysical properties of three 26-pendant zinc porphyrin polymers have been measured in fluid media and in thin films and have been compared with those of their corresponding β-substituted monomers and the model metalloporphyrin, ZnTPP. The styrene-tethered monomers and the ether-tethered monomer behave in a qualitatively similar fashion;

conjugation of the tether with the macrocycle makes little difference. The substituted monomers all exhibit properties that are consistent with small increases in the radiationless decay rates of the electronically excited S_2 and S_1 states compared with the unsubstituted model, ZnTPP. Otherwise the monomers and ZnTPP behave similarly; monoexponential singlet relaxation rates, large yields of triplet, and small yields of upconverted S_2 emission following TTA in degassed media are observed.

Although all three polymers behave in a qualitatively similar fashion, they exhibit important differences compared with the set of three substituted monomers that serve as their pendants. S_2 and S_1 fluorescence quantum yields are smaller; S_1 fluorescence decays are bi-exponential; triplet yields are much smaller; two additional rapid kinetically pseudo-first order triplet decay processes are observed. Rather than producing a near quantitative yield of triplets by intersystem crossing from S_1 (as seen in the monomers), both the S_2 and particularly the S_1 states of the polymers decay directly to the ground state. These differences are consistent with the structures of the polymers and a consequence of dynamic exciton quenching processes occurring during the lifetimes of the electronically excited polymer species.

Consistent with the lack of excitonic splitting in their absorption spectra, the major decay routes of the initially excited polymers are attributed to dynamic processes – internal self-quenching of the excited singlets – occurring after electronic excitation. A small subset of initially excited polymers behaves like the monomers from which they are derived (*e.g.* 1.5 ns S_1 fluorescence decay and 240 μs triplet lifetimes), and this subset is assigned to molecules in which the exciton is confined to a single porphyrin pendant that interacts only with the surrounding solvent medium during its lifetime. A much larger fraction of singlet excited

polymer decays directly to the ground state. During a polymer's S_1 nanosecond lifetime, internal rotation of pendants about the polymer backbone can bring two adjacent porphyrins into electronic contact. Self-quenching by an excimeric mechanism is the result. A rapid (microsecond or sub-microsecond) decay process in a tiny minority of triplet states is a collateral consequence of this excimeric interaction. A third pseudo-first order process is also observed – perhaps accompanying self-quenching by large-amplitude motion of a single chain or by interchain interactions involving two convoluted polymer molecules. In any case, the yield of triplet states in the polymers is so small that intermolecular TTA contributes nothing observable to their overall triplet decay kinetics.

TTA can be observed in both fluid solutions and thin films, but the linear power dependence of the extremely weak S_2 emission of the degassed polymers in all media (upconverted fluorescence quantum yield of the order of 10^{-7}) is unique. The upconverted emission intensity is reduced to zero in air, proving that triplets are involved, but its linear power dependence in degassed media suggests that the mechanism must be entirely different from the kinetically second order interspecies annihilation that occurs with the monomers and ZnTPP. The mechanism by which this linear power dependence is produced will be pursued in future experiments. For the present we can conclude that, irrespective of mechanism, the small yields of triplets and the tiny upconversion quantum yields demonstrate that polymers with freely moving porphyrin pendants such as these are not suitable for use as upconverters in photovoltaic or electroluminescent devices. Further synthetic control of the polymer structure to restrict mobility and excimeric interactions of the pendant porphyrin chromophores is one strategy that might address the low upconversion yields.

Supporting Information:

The Supporting Information is available free of charge on the ACS Publications website at DOI: 10.1021/jacsxxxxxxx.

Detailed synthesis and characterization procedures, detailed description of photophysical instrumentation and measurement procedures, absorption and fluorescence spectra, S1 fluorescence decay profiles, upconversion power dependences, transient triplet spectra, monomer transient triplet decays on a microsecond time scale, quantum yields of S_2 fluorescence resulting from non-coherent photon upconversion by triplet-triplet annihilation. (PDF).

Acknowledgements:

The authors are pleased to acknowledge the Natural Sciences and Engineering Research Council of Canada and the Australian Research Council Centre of Excellence in Exciton Science (CE170100026) for their continuing financial support. The Saskatchewan Structural Science Centre provided equipment and technical assistance. Phillip Boutin and Neeraj Joshi are thanked for their preliminary work on this project. A. L. S. thanks the University of Saskatchewan and the College of Arts and Science for partial financial support. W. W. H. W. was supported by an Australian Research Council Future Fellowship (FT130100500). This work was made possible by support from the Australian Renewable Energy Agency which funds the project grants within the Australian Centre for Advanced Photovoltaics (ACAP). Responsibility

for the views, information or advice expressed herein is not accepted by the Australian Government.

References:

(1) Ostroverkhova, O. Organic optoelectronic materials: mechanisms and applications, *Chem. Rev.* **2016**, *116*, 13714-13751.

(2) Wang, L.; Long, R.; Prezhdo, O. V. Time-domain *ab initio* modeling of photoinduced dynamics at nanoscale interfaces, *Ann. Rev. Phys. Chem.* **2015**, *66*, 549-579.

(3) Pu, C.; Qin, H.; Gao, Y.; Zhou, J.; Wang, P.; Peng, X. Synthetic control of exciton behavior in colloidal quantum dots, *J. Amer. Chem. Soc.* **2017**, *139*, 3302-3311.

(4) Ghimire, S.; Biju, V. Relations of exciton dynamics in quantum dots to photoluminescence, lasing and energy harvesting, *J. Photochem. Photobiol. C, Photochem. Rev.* **2018**, *34*, 137-151.

(5) Jiang, Y.; McNeill J. Light-harvesting and amplified energy transfer in conjugated polymer nanoparticles, *Chem. Rev.* **2017**, *117*, 838-859.

(6) Ingram, G. L.; Lu, Z-H. Design principles for highly efficient organic light-emitting diodes, *J. Photon. Energy* **2014**, *4*, 040993.

(7) Petrone, A.; Lingerfelt, D. B.; Rega, N.; Li, X. From charge-transfer to a charge-separated state: a perspective from the real-time TDDFT excitonic dynamics**,** *Phys. Chem. Chem. Phys.* **2014**, *16*, 24457-24465.

(8) Drain, C. M.; Varotto, A.; Radivojevic, I. Self-organized porphyrinic materials, *Chem. Rev.* **2009**, *109*, 1630–1658.

(9) Steer, R. P. Prospects for efficient solar energy upconversion using metalloporphyrins as dual absorber-upconverters, *RSC Dalton Trans*. **2018**, *47*, 8517-8525.

(10) Carmichael, I.; Hug, G. L. Triplet–triplet absorption spectra of organic molecules in condensed phases, *J. Phys. Chem. Ref. Data* **1986**, *15*, 1-240.

(11) Steer, R. P. Concerning the correct and incorrect assignments of Soret (S_2-S_0) fluorescence in porphyrinoids: a short critical review, *Photochem. Photobiol. Sci.* **2014**, *13*, 1117-1122.

(12) Papkovsky, D. B.; O'Riordan, T. C., Emerging applications of phosphorescent metalloporphyrins, *J. Fluorescence* **2005**, *15*, 569-584.

(13) Tanaka, T.; Osuka, A. Chemistry of *meso*-aryl-substituted expanded porphyrins: aromaticity and molecular twist, *Chem. Rev.* **2017**, *117*, 2584−2640.

(14) Day, N. U.; Wamsera, C. C.; Walter, M. G. Porphyrin polymers and organic frameworks, *Polym. Int.* **2015**, *64*, 833–857.

(15) Cho, H. S.; Jeong, D. H.; Cho, S.; Kim, D.; Matsuzaki, Y.; Tanaka, K.; Tsuda, A.; Osuka, A. Photophysical properties of porphyrin tapes, *J. Amer. Chem. Soc.* **2002**, *124*, 14642-14654.

(16) Jeong, Y-H.; Yoon, H-J.; Jang, W-D. Dendrimer porphyrin-based self-assembled nano-devices for biomedical applications, *Polymer J.* **2012**, *44*, 512-521.

(17) Lin, N-T.; Satyanarayana, K.; Chen, C-H.; Tsai, Y-F.; Yu, S. S-F.; Chan, S. I.; Luh, T-Y. Controlling the orientation of pendants in two-dimensional comb-Like polymers by varying stiffness of polymeric backbones, *Macromolecules* **2014**, *47*, 6166−6172.

(18) Fujitsuka, M.; Okada, A.; Tojo, S.; Takei, F.; Onitsuka, K.; Takahashi, S.; Majima, T. Rapid exciton migration and fluorescent energy transfer in helical polyisocyanides with regularly arranged porphyrin pendants, *J. Phys. Chem. B* **2004**, *108*, 11935-11941.

(19) Fujitsuka, M.; Satyanarayanab, K.; Luh, T-Y.; Majima, T. Singlet–singlet and singlet–triplet annihilations in structure-regulated porphyrin polymers, *J. Photochem. Photobiol. A, Chem.* **2016**, *331*, 56-59.

(20) Steer, R. P. Electronic energy pooling in organic systems: a cross-disciplinary tutorial review, *Can. J. Chem.* **2017**, *95*, 1025-1040.

(21) Manna, M. K.; Shokri, S.; Wiederrecht, G. P.; Gosztola, D. J.; Ayitou, A. J-L. New perspectives for triplet–triplet annihilation based photon upconversion using all-organic energy donor and acceptor chromophores, *Chem. Commun.* **2018**, *54*, 5809-5818.

(22) Rautela, R.; Joshi, N. K.; Novakovic, S.; Wong, W. W. H.; White, J. M.; Ghiggino, K. P.; Paige, M. F.; Steer, R. P. Determinants of the efficiency of photon upconversion by triplet-triplet annihilation in the solid state: zinc porphyrin derivatives in PVA. *Phys. Chem. Chem. Phys.* **2017**, *19*, 23471-23482.

(23) Stevens, A. L.; Joshi, N. K.; Paige, M. F.; Steer, R. P. Photophysics of zinc porphyrin aggregates in dilute water-ethanol solutions. *J. Phys. Chem. B* **2017**, *121*, 11180-11188.

(24) Tilley, A. J.; Robotham, B. E.; Steer, R. P.; Ghiggino, K. P. Sensitized non-coherent photon upconversion by intramolecular triplet–triplet annihilation in a diphenylanthracene pendant polymer, *Chem. Phys. Lett.* **2014**, *618*, 198-202.

(25) Boutin, P. C.; Ghiggino, K. P.; Kelly, T. L.; Steer, R. P. Photon upconversion by triplet−triplet annihilation in $Ru(bpy)_3$-and DPA-functionalized polymers, *J. Phys. Chem. Lett.* **2013**, *4*, 4113-4118.

(26) Tilley, A. J.; Chen, M.; Danczak, S. M.; Ghiggino, K. P.; White, J. M. Electronic energy transfer in pendant MEH-PPV polymers, *Polym. Chem.* **2012,** *3*, 892-899.

(27) Boutin, P. C.; Ghiggino, K. P.; Kelly, T. L.; Steer, R. P. Photon upconversion by triplet−triplet annihilation in $Ru(bpy)_3$-and DPA-functionalized polymers, *J. Phys. Chem. Lett.* **2013**, *4*, 4113-4118. Supporting Information.

(28) Tripathy, U.; Kowalska, D.; Liu, X.; Velate, S.; Steer, R. P. Photophysics of Soret-excited tetrapyrroles in solution. I. MgTPP, ZnTPP, CdTPP, *J. Phys. Chem. A* **2008**, *112*, 5824-5833.

(29) Sugunan, S. K.; Tripathy, U.; Brunet, S. M. K.; Paige, M. F.; Steer, R. P. Mechanisms of low-power noncoherent photon upconversion in metalloporphyrin-organic blue emitter systems in solution. *J. Phys. Chem. A* **2009**, *113*, 8548-8556.

(30) Kowalska, D.; Steer, R. P. Quenching of MgTPP and ZnTPP fluorescence by molecular oxygen *J. Photochem. Photobiol. A* **2008**, *195*, 223-227.

(31) Nathanael, J. G.; Hancock, A. N.; Wille, U. Reaction of amino acids, di- and tripeptides with the environmental oxidant $NO_{3\bullet}$: A laser flash photolysis and computational study, *Chem. Asian J.* **2016,** *11*, 3188-3195.

(32) Karolczak, J.; Kowalska, D.; Lukaszewicz, A.; Maciejewski, A.; Steer, R. P. Photophysical studies of porphyrins and metalloporphyrins: accurate measurements of fluorescence spectra and fluorescence quantum yields for Soret band excitation of zinc tetraphenylporphyrin *J. Phys. Chem. A* **2004**, *108*, 4570-4575.

(33) D. F. Stel'makh and M. P. Tsvirko, Determination of formation probabilities of excited states during triplet-triplet annihilation, *Zh. Prikl. Spektrosk.*, **1982**, *36*, 606-619.

(34) Hurley, J. K.; Sinai, N.; Linschitz, H. Actinometry in monochromatic flash photolysis: the extinction coefficient of triplet benzophenone and quantum yield of triplet zinc tetraphenyl porphyrin, *Photochem Photobiol.* **1983**, *38*, 9-14.

(35) Ventura, B.; Flamigni, L.; Marconi, G.; Lodato, F.; Officer, D.L. Extending the porphyrin core: synthesis and photophysical characterization of porphyrins with π-conjugated β-substituents, *New J. Chem.* **2007**, *32*, 166-178.

(36) Fox, M. A.; Britt, P. F. Photophysics of 10-substituted poly(2-(9-anthryl)ethyl methacrylates), *Macromolecules* **1990**, *23*, 4533-4542.

(37) O'Brien, J. A.; Rallabandi, S.; Tripathy, U.; Paige, M. F.; Steer, R.P. Efficient S_2 state production in ZnTPP–PMMA thin films by triplet–triplet annihilation: Evidence of solute aggregation in photon upconversion systems, *Chem. Phys. Lett.* **2009**, *475*, 220-222.